

Linking Microscopic Reversibility to Macroscopic Irreversibility, Emphasizing the Role of Deterministic Thermostats and Simple Examples, At and Away from Equilibrium

Wm. G. Hoover and Carol G. Hoover

Ruby Valley Research Institute

Highway Contract 60, Box 601

Ruby Valley, Nevada 89833

(Dated: May 22, 2018)

Abstract

Molecular Dynamics and Statistical Mechanics make possible a particle-based understanding of Thermodynamics and Hydrodynamics, including the fascinating Loschmidt contradiction between time-reversible atomistic mechanics and the time-irreversible thermodynamic dissipation incorporated into macroscopic fluid and solid mechanics.

PACS numbers: 05.20.-y, 05.45.-a, 05.70.Ln, 07.05.Tp, 44.10.+i

Keywords: Reversibility, Lyapunov Instability, Shockwaves, Liouville's Theorems

I. INTRODUCTION

Among the many problem areas in mechanics the study of instabilities and irreversible processes seem particularly interesting. Engineering mechanics exists as a discipline because failures of structures cost so many lives. The analysis of local Lyapunov instability gives a means for localizing and predicting catastrophic failures so that there is a decidedly practical engineering aspect of this fascinating scientific research area.

The goal we pursue here is to develop models that help us to understand. It is profoundly interesting that the small scale microscopic models of material behavior (ordinary Newtonian mechanics) are time-reversible while the macroscopic models of the same thing (finite-element and finite-difference fluid mechanics and solid mechanics) are irreversible. The tools from nonlinear dynamics and chaos are useful in analyzing these two kinds of description.

Here we describe the basic building blocks for particle simulation and point out the ways that these time-reversible simulations already lead to time-irreversible behavior. Most of the examples treated here are also described in our three books on computational statistical mechanics, smooth-particle applied mechanics, and time reversibility, computer simulation, algorithms, and chaos¹⁻³.

II. ALGORITHM FOR CONSERVATIVE PARTICLE MECHANICS

No special tricks are necessary to get started with particle-based simulations. Microscopic mechanics can provide us with accurate particle trajectories $\{ q(t) \}$. All we need to do is to integrate Newton's ordinary differential equations of motion ,

$$\{ m\ddot{q} = F(q) = -\nabla\Phi \} .$$

Here Φ is the potential energy, a function of the coordinates $\{ q \}$. Alternatively, we can obtain an equivalent coordinate-momentum description $\{ q(t), p(t) \}$ by integrating Hamilton's first-order ordinary differential equations :

$$\{ \dot{q} = +(\partial\mathcal{H}/\partial p) ; \dot{p} = -(\partial\mathcal{H}/\partial q) \} .$$

Both these approaches are time-reversible. That is, a movie of the motion, played backwards, satisfies exactly the *same* equations (with the values of q and p in reversed order and with

the sign of p changed also). A movie is an excellent analog of numerical simulation. Both the simulation and the movie are sets of discrete records of coordinates at discrete values of the time, separated by the “timestep” Δt . In addition to the basic algorithm keep in mind that three crucial questions remain to be answered: [1] what are the initial conditions, [2] what are the boundary conditions, and (most important of all) [3] what is the problem to be solved?

Macroscopic continuum mechanics is based on the three conservation laws for mass, momentum, and energy :

$$\dot{\rho} = -\rho \nabla \cdot u ; \quad \rho \dot{u} = -\nabla \cdot P ; \quad \rho \dot{e} = -\nabla u : P - \nabla \cdot Q .$$

Here ρ is density, u is velocity, e is energy per unit mass, P is the pressure tensor (force per unit area, necessarily a symmetric second-rank tensor), and Q is the heat flux vector (energy flow per unit area). All these variables are continuous functions of space and time. Both P and Q , as well as $\dot{\rho}$, \dot{u} , and \dot{e} , are defined in the *comoving* frame, a coordinate frame moving with the local velocity $u(r, t)$. Finite-difference approximations to the gradients on the righthand sides of the three continuum equations, evaluated at a discrete set of spatial mesh points, reduce the partial differential equations to ordinary ones, which can then be solved with Runge-Kutta integration. Again, the hard part of the problem is the same: what to do and how to implement the initial and boundary conditions.

Different materials can be described by different types of constitutive relations (elastic, plastic, viscous, ...) giving P and Q in terms of the basic $\{ \rho, u, e \}$ set, together with their time derivatives and spatial gradients. Time-reversed movies of solved macroscopic problems look “funny” and make no sense. This is because the underlying phenomenological constitutive relations are typically irreversible. The simplest most familiar irreversible examples are Newtonian viscosity and Fourier heat conduction :

$$P = [P_{\text{eq}} - \lambda \nabla \cdot u] I - \eta [\nabla u + \nabla u^t] ; \quad Q = -\kappa \nabla T .$$

In the symmetrized velocity gradient ∇u^t is the transpose of ∇u . I is the unit tensor. A boxed conducting fluid, with that fluid initially in motion, (a Rayleigh-Bénard flow, for instance, but with the box suddenly insulated and with the accelerating gravitational field suddenly switched off) described with a shear viscosity η and a heat conductivity κ eventually comes to an isothermal state of rest. Evidently the reversed movie of this decay

makes no sense and would correspond to an illegal “something from nothing” contradicting the Second Law of Thermodynamics. Of course, with the right initial conditions and the right boundary conditions, one can indeed observe tornadoes! For an $L \times L$ (two-dimensional) system, with kinematic viscosity and thermal diffusivity of order D the initial gradients decay exponentially, $\simeq e^{-Dt/L^2}$. The reversed movie, with its exponential growth, $\simeq e^{+Dt/L^2}$, is simply wrong.

In applications of mechanics to simulation we strongly recommend the use of the fourth-order Runge-Kutta integrator because it is easy to use and to modify for the treatment of open systems interacting with their environments. If the focus is on the time-reversibility of conservative Newtonian systems it is useful to consider a very simple, yet rigorously time-reversible, integrator discovered by Levesque and Verlet⁴. In order better to understand the coexistence of the reversible microscopic and irreversible macroscopic views we adopt Levesque and Verlet’s “bit-reversible” algorithm. This approach generates a numerical trajectory in an *integer* coordinate space, by rounding off the acceleration terms :

$$\{ q_{n+1} - 2q_n + q_{n-1} = [(F(q_n)(\Delta t)^2/m]_{\text{integer}} \} .$$

The subscripts indicate the time, in units of the (integer) timestep Δt . The initial conditions to start this algorithm are the coordinates at two successive times.

A simple illustration of the algorithm follows a harmonic oscillator trajectory, using unit mass, force constant, and timestep Δt :

$$q_+ - 2q_0 + q_- = -q_0 \longrightarrow q_+ \equiv q_0 - q_- .$$

The solution of repeating coordinates $\{ +1, +1, 0, -1, -1, 0, \dots \}$, is typical, and illustrates the fact that no matter what the initial conditions, the solution is both periodic (for chaotic problems, the length of the period is of order the square root of the number of states) and reversible. The algorithm is a faithful analog of classical deterministic time-reversible mechanics. If momenta are desired they too can be approximated accurately from the coordinate values :

$$p_0 \equiv \left[\frac{4}{3} \right] \frac{(q_+ - q_-)}{2\Delta t} - \left[\frac{1}{3} \right] \frac{(q_{++} - q_{--})}{4\Delta t} .$$

Figure 1 compares the energy calculated with these momenta with calculations based on the Beeman and velocity-Verlet algorithms. Our formulation (small dots in the Figure) is clearly an improvement. It is evident that a promising research area lies in the development

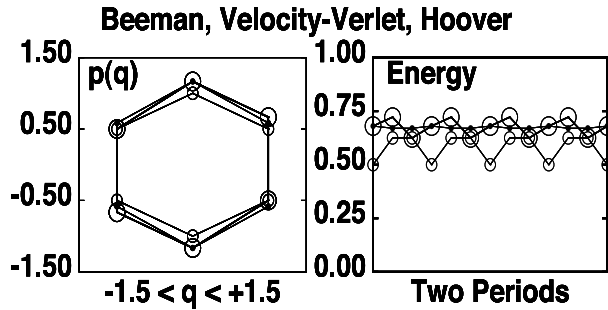


FIG. 1: The Beeman and Velocity-Verlet approximations to the harmonic oscillator momentum are compared with the more nearly accurate formula given in the text (at the left). The corresponding total energies are shown at the right over two oscillations with $\Delta t = 1$. The approximation mentioned in the text is the best of the three and corresponds to the smallest dots.

of higher-order bit-reversible algorithms combining coordinates, velocities, and accelerations from more than three successive times.

III. IRREVERSIBILITY FROM TIME-REVERSIBLE MOTION EQUATIONS?

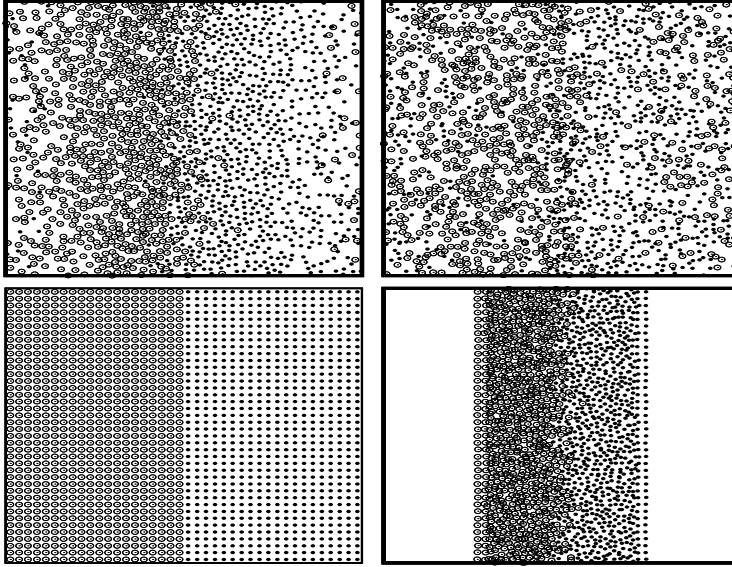
Is there any chance of detecting *irreversibility* with such a time-reversible algorithm? Oddly enough, there is! It is based on the analysis of Lyapunov instability, looking in the *neighborhood* of the trajectory, not just at the trajectory itself. Such a nonlocal analysis necessarily depends upon the imagination and the information contributed by an observer of the motion. Let us take an example, a *maximally irreversible* situation described by time-reversible, even bit-reversible, Newtonian mechanics. Consider the pair of shockwaves launched by the collision of two mirror-image fluid samples. See Figure 2 for four snapshots of such a problem. *Initially* the velocities are $\pm u$. *Eventually* the periodic $L \times L$ system shows no more systematic motion – the initial kinetic energy has been completely converted to internal energy (heat) :

$$(u^2/2) \rightarrow e .$$

Just as before, any portion of the developing trajectory can be reversed precisely and exactly despite the Lyapunov instability (exponential growth of perturbations) of the dynamics.

There is a vast literature⁵⁻⁹ on the quantification of Lyapunov instability, the exponen-

Times 0, 11.5, 23.0, 46.00



Twofold Compression with N=1600

FIG. 2: Snapshots from the twofold compression of a 40×40 cold crystal with unit density and with the pair potential $\phi = (1 - r^2)^4$. Initially half the particles move to the right and half to the left, at speed 0.875. The second snapshot, time = 11.5, and located at bottom right, corresponds to the maximum twofold compression. Such “irreversible” motions can be reversed precisely, for as long as desired, with the Levesque-Verlet bit-reversible integration algorithm.

tially sensitive deformation of comoving hypervolumes in q space, p space, or $\{q, p\}$ phase space. For N particles in two dimensions the $4N$ -dimensional phase-space motion defines $4N$ local Lyapunov exponents. The fact that these “local” exponents depend upon the chosen coordinate system can be viewed as a disadvantage or as an opportunity. Again, there are many promising research problems suggested by this observation. Optimizing the analysis is certainly a useful and stimulating activity.

The largest Lyapunov exponent – we will call it $\lambda_1(t)$ – associated with the motion can be found by following two nearby trajectories in time. The primary or “reference” trajectory can be generated with bit-reversible dynamics, so that it is possible to extend it as far as desired into the future or the past⁷. The dynamics of a nearby “satellite” trajectory is restricted by constraining the satellite trajectory to stay within a fixed distance of the

reference trajectory. The satellite dynamics can readily be generated with Runge-Kutta integration, rescaling the separation between the two trajectories at the end of each time step. The local Lyapunov exponent is :

$$\lambda_1(t) \equiv \left[\frac{1}{\Delta t} \right] \ln \left[\frac{(\Delta r)_{\text{before}}}{(\Delta r)_{\text{after}}} \right] ; \Delta r \equiv |r_{\text{satellite}} - r_{\text{reference}}| .$$

Although the motion equations are perfectly reversible for both the reference and the satellite, the reversed satellite trajectory turns out to be totally unlike the forward one, *if* the system is a nonequilibrium system. Both the local Lyapunov exponent associated with the instability and the identities of those particles making above-average contributions to the offset vector separating the trajectories , $\Delta r \equiv r_{\text{satellite}} - r_{\text{reference}}$, are qualitatively different. In a typical shockwave simulation of the type shown in Figure 2 the number of these more-heavily-weighted particles is about twice as great in the reversed motion as in the forward one.

This is an extremely interesting result. No doubt it suggests various “Arrows of Time” which can be constructed based on the structure of nearby trajectories (which react to the past, not the future). A study of irreversible flows from this standpoint should shed light on the reversibility paradox for simple Newtonian and Hamiltonian systems.

IV. IRREVERSIBILITY FOR TIME-REVERSIBLE “OPEN” SYSTEMS

In order to control nonequilibrium states, in particular nonequilibrium *steady* states, it is necessary to do work and/or to exchange heat, with the system of interest. The dynamics becomes a little more complicated due to these interactions, but the interpretation compensates by becoming simpler. Here we take up the description of “open systems”.

A. Microscopic Pressure, Heat Flux, and Temperature

“Open” systems have mechanical and/or thermal connections to their environment, opening up the possibility of simulating processes including thermodynamic work and the flow of heat. Analysis of these systems requires microscopic analogs for all the continuum variables. Density, velocity, and energy are the simplest of these. We adopt the smooth-particle

averaging method discovered by Lucy and Monaghan in 1977^{10,11} :

$$\rho(r, t) \equiv \sum_i m_i w(r - r_i) ; \rho(r, t)u(r, t) \equiv \sum_i m_i v_i w(r - r_i) ; \rho(r, t)e(r, t) \equiv \sum_i m_i e_i w(r - r_i) .$$

The particle energies $\{ e_i \}$ are necessarily defined in the comoving frame, which moves with velocity $u(r, t)$. A useful weight function, with a range h which can be optimized, is Lucy's, here normalized for two space dimensions :

$$w(r) = (5/\pi h^2)(1 + 3z)(1 - z)^3 \quad z \equiv |r|/h .$$

This weight-function approach guarantees the continuity of the first and second spatial derivatives of the field variables and lends itself to optimization studies.

In addition to the basic mass, momentum, and energy, several other variables need to be considered in order to compare microscopic and macroscopic simulations. Unlike their continuum cousins, the pressure tensor and the heat flux vector from molecular dynamics are respectively even and odd functions of the time :

$$PV = \sum_{\text{pairs}} (rF)_{ij} + \sum_i (pp/m)_i ; \quad QV = \sum_{\text{pairs}} r_{ij} [F_{ij} \cdot (p_i + p_j)/2] + \sum_i (ep/m)_i .$$

Here $r_{ij} \equiv r_i - r_j$ and F_{ij} is the force on Particle i due to its interaction with Particle j . The individual particle energies $\{ e_i \}$ include half of each particle's pair interactions with its neighbors.

Temperature needs a definition too. The usual equilibrium definition, based on entropy, is useless away from equilibrium where entropy has no consistent definition^{1,2}. *At equilibrium* *Temperature* can be defined in many ways, all based on Gibbs' statistical mechanics or Maxwell and Boltzmann's kinetic theory. The even moments of the velocity distribution are examples. In addition to these there are also configurational definitions. The simplest "configurational temperature" is based on an identity from Landau and Lifshitz' text^{12,13} :

$$kT = \frac{\langle (\nabla \mathcal{H})^2 \rangle}{\langle \nabla^2 \mathcal{H} \rangle} .$$

This definition follows from an integration by parts in Gibbs' canonical ensemble. If the differentiation indicated by ∇ is carried out in momentum space the Landau-Lifshitz formula gives the usual kinetic-theory definition of temperature , $mkT_{xx} = \langle p_x^2 \rangle$. If instead the gradient is carried out in coordinate space the "configurational temperature" depends on the first and second derivatives of the potential function governing the motion :

$$kT_{\text{configurational}} \equiv \langle F^2 \rangle / \langle \nabla^2 \Phi \rangle .$$

One-body or many-body configurational temperatures, either scalar or tensor, can be defined in this way. But an evaluation of them for the shockwave problem reveals divergences. Typically particle values of $\nabla^2\Phi$ frequently alternate between positive or negative values, so that the corresponding configurational temperatures frequently diverge! Configurational temperature also has unphysical undesirable contributions arising from rotation whenever Coriolis' or centrifugal forces are significant.

The simplest definition for temperature is the kinetic second-moment one. It is based on a mechanical model of a working ideal-gas thermometer. In that instance a relatively heavy mass- M "system atom" interacts with a collection of light-weight mass- m "ideal-gas thermometer" particles characterized by an unchanging equilibrium Maxwell-Boltzmann distribution with temperature T . Kinetic theory shows that the averaged effect of such collisions causes the system-atom velocity to decay while its mean-squared velocity approaches the equilibrium value for the temperature T :

$$\langle \dot{v}_x \rangle \propto -(v_x/\tau) ; \langle \dot{v}_x v_x \rangle \propto [(kT_{xx}/m) - v_x^2]/\tau ; [\text{for } m \ll M] .$$

Accordingly, we adopt the kinetic definition of temperature in what follows. With temperature defined we can proceed to devise "thermostats" able to control it.

B. Time-Reversible Deterministic Thermostats

The first of the deterministic mechanical thermostats was Woodcock's isokinetic thermostat¹⁴, implemented by rescaling the velocities at the end of each timestep. Much later it was discovered^{15,16} that a continuous time-reversible version of this thermostat could be implemented with a *time-reversible* friction coefficient ζ :

$$\dot{p} = F(q) - \zeta p ; \zeta = \sum (F \cdot p) / \sum (p^2/m) \rightarrow (d/dt) \sum (p^2/m) \equiv 0 .$$

This "isokinetic" thermostat can be applied to one or many particles and to one or many space directions.

An illustrative application is the "Galton Board"^{1,2,15}, in which a single particle is accelerated through a lattice of scatterers but constrained to move at constant speed. Overall, the potential energy drops. Because the mean value of the friction coefficient is necessarily positive, the phase-space probability density collapses onto a multifractal strange attractor,

quantifying the rarity of nonequilibrium phase-space states. This approach to temperature control is often termed the “Gaussian” thermostat because Gauss’ Principle (of Least Constraint) gives this thermostat when applied to the problem of constraining the kinetic energy¹⁶. Reference 15 is a detailed discussion of the model (summarized in References 1 and 2). This work clearly shows the fractal nature of the phase space (with vanishing phase volume) that results when the dynamics is thermostated. Fancier thermostats, based on statistical mechanics, can be found.

In 1984 Shuichi Nosé discovered a precursor of the best of them, a thermostat¹⁷ with a more elaborate basis in Lagrangian and Hamiltonian mechanics, but somewhat disfigured by a novel “time-scaling variable” $s \equiv dt_{\text{old}}/dt_{\text{new}}$. His thermostat imposed Gibbs’ canonical phase space distribution at equilibrium rather than the less-usual isokinetic one. A simplification of his equation of motion, without the useless time-scaling, likewise contained a friction coefficient, which itself obeyed an evolution equation depending upon *past* values of the kinetic energy :

$$\{ \dot{p} = F(q) - \zeta p \} ; \dot{\zeta} = [(T(\{p\})/T_0) - 1] / \tau^2 \text{ [Nosé - Hoover]} .$$

The relaxation time τ is a free parameter determining the time required for the thermostat forces $\{-\zeta p\}$ to bring the kinetic temperature $T(\{p\})$ to the desired thermostat temperature T_0 . Just as in the isokinetic case the nonequilibrium averaged friction coefficient for this “Nosé-Hoover” mechanics is positive, leading once again to multifractal phase space distributions away from equilibrium. There is an extensive somewhat mathematical literature having to do with picking the “right” relaxation time or the “right” thermostat.

The Gaussian and Nosé-Hoover thermostats are particularly useful for controlling nonequilibrium problems, such as shear flows and heat flows, and the Rayleigh-Bénard problem combining them. The definition of temperature depends upon the definition of the local velocity $u(r, t)$. A straightforward definition of velocity, which nicely satisfies the continuity equation exactly³, can be based on smooth-particle weighting functions :

$$u(r, t) \equiv \sum_i v_i w(|r - r_i|) / \sum_i w(|r - r_i|) .$$

The Gauss, Nosé, and Nosé-Hoover thermostats can *all* be related to Hamiltonian mechanics. Dettmann, together with Morriss, carried out much of this work, with later contributions by Bond, Laird, and Leimkuhler, and then by Campisi, Hänggi, Talkner, and

Zhan¹⁸⁻²¹. All of them helped to clarify the connections of time-reversible thermostats with standard Hamiltonian mechanics. This work leads to the conclusion that *many* different thermostats can be used at equilibrium but that some of them fail in nonequilibrium situations, even in situations close to equilibrium. Just as in real life the failures, rather than the successes, are the more newsworthy subjects. Let us turn to some examples.

C. Thermostat Failures – Oscillators, Heat Conduction, and the ϕ^4 Model

A very stimulating “log-thermostat” has just been described by Campisi, Hänggi, Talkner, and Zhan²¹. They pointed out that the microcanonical (constant energy) ensemble distribution for a logarithmic potential generates (at least formally) the Maxwell-Boltzmann velocity distribution :

$$\phi \equiv kT \ln q \rightarrow \int_0^{+\infty} dq \delta[2H_0 - kT \ln q^2 - (p^2/m)] \propto \exp[(H_0/kT) - (p^2/2mkT)]$$

Because the dynamics of this thermostat is unstable, there being nothing to keep q away from the origin, in applications they recommend using $kT \ln(q^2 + \delta^2)$, where δ is sufficiently small.

Our effort to use this thermostat for a nonequilibrium heat flow problem failed. Connecting a cold and a hot log-thermostat to opposite ends of a two-particle ϕ^4 chain gave different temperatures at the two ends, but *no heat flux at all*. The problem is that the Hamiltonian log-thermostat is unable to replicate the phase-space contraction associated with dissipative systems. There are some other examples of such failures. Leete and Hoover’s Hamiltonian^{22,23} ,

$$\mathcal{H}_{\text{HL}} = \sqrt{4K(p)K_0 + \Phi(q)} - K_0 ,$$

keeps the kinetic energy, $\sum(m\dot{q}^2/2)$ constant, equal to K_0 . The *configurational* temperature can alternatively be kept constant using a special Hamiltonian. In both these cases a cold and a hot thermostated region, in contact with Newtonian regions, gives *no heat flux at all* despite huge temperature differences. The lesson is that Hamiltonian mechanics is not able to describe dissipation properly.

V. THERMOSTAT SUCCESSES” OSCILLATORS AND COMPLEX SYSTEMS

A “good” thermostat should, for instance, be able to provide good solutions of the Rayleigh-Bénard problem, heat transfer through a compressible fluid in a gravitational field. It should also be useful in treating small-scale “toy problems”. The simplest thermostat test problems are [1] a harmonic oscillator²⁴ with a coordinate-dependent temperature :

$$T(q) = 1 + \epsilon \tanh(q) ;$$

and [2] the flow of heat through a ϕ^4 chain of particles :

$$\mathcal{H} \equiv \sum_i [(p_i^2/2m) + (\delta x_i^4/4)] + \sum_{i < j} \phi_{ij} ,$$

where ϕ is a nearest-neighbor Hooke’s-Law potential and where the first few and last few particles in the chain are thermostated with a Gaussian or Nosé-Hoover or another thermostat. This model is a specially good one to study because it is known to satisfy Fourier’s law, even in one dimension. A comparison of seven different thermostat methods showed that the ϕ^4 problem is well-posed and relatively easy to solve²⁵.

Some Hamiltonian-based thermostats are ineffective for nonequilibrium problems^{21–23} and it is useful to understand why. At equilibrium a given temperature and volume imply corresponding values of the kinetic and potential energies. This is also true for particular states away from equilibrium, even where there is no longer a unique equation-of-state relation. Using a Hamiltonian thermostat away from equilibrium one can independently specify the kinetic energy *and* the potential energy or the temperature *and* the energy. This additional freedom contradicts the notion of thermodynamic state and can lead to very strange results²³. Constraining the configurational temperature or using a version of Hamiltonian mechanics to constrain the kinetic energy discovered by Hoover and Leete provide temperature profiles that make no sense. The log-thermostat is another demonstration that Hamiltonian mechanics is a poor choice for thermostats. This paradoxical situation is the symptom of two incompatible requirements on the dynamics: [1] Liouville’s Theorem requires that the phase-space motion be incompressible; [2] Heat flow consistent with the Second Law of Thermodynamics requires that the phase volume decrease to zero.

Several of the thermostats have no problem with generating heat flows and solve the problem of decreasing phase volume by generating strange attractors in the phase space.

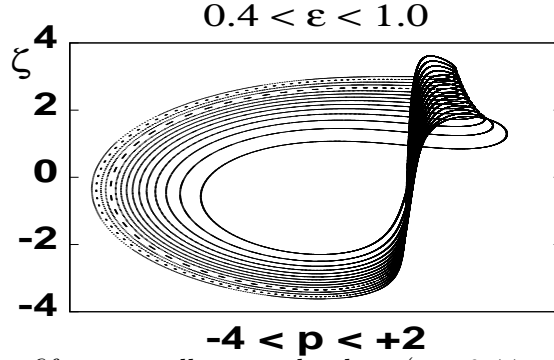


FIG. 3: $\zeta(p)$ is plotted for fifteen equally-spaced values ($\epsilon = 0.44$ to 1.00) of the maximum temperature gradient for the (q, p, ζ) nonequilibrium Nosé-Hoover oscillator. All these data correspond to fully-converged limit cycles.

Let us consider what might appear to be the simplest of these problems, the Nosé-Hoover oscillator²⁴ with a temperature gradient¹ :

$$\dot{q} = p ; \dot{p} = -q - \zeta p ; \dot{\zeta} = p^2 - T(q) ; T(q) = 1 + \epsilon \tanh(q) ; 0 < \epsilon < 1 .$$

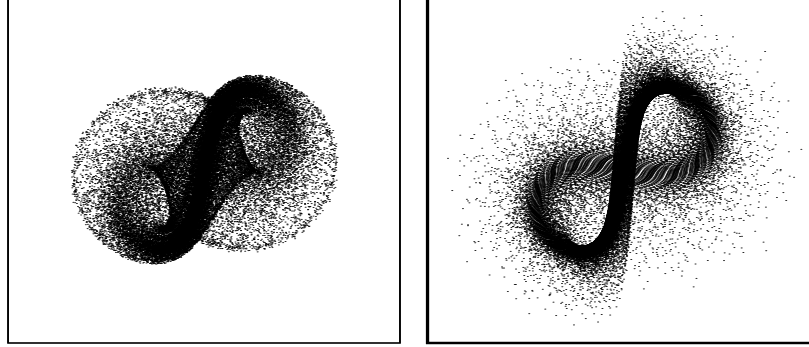
For $\epsilon > 0.4$ the motion is a one-dimensional limit cycle with $\langle \zeta \rangle$ positive. The mean value of the friction coefficient ζ in the range $(0.44 < \epsilon < 1.0)$ increases from about 0.15 to 1.35 . Figure 3 shows the gradual expansion of the hysteretic limit cycle as the maximum temperature gradient is increased from 0.44 to 1.00 .

Figures 4 and 5 show a bit of the complexity associated with smaller values of the temperature gradient. Using an initial momentum of unity gives more regular attractors, of the type shown to the left. On the other hand, much higher initial momenta give chaotic distributions like those shown to the right. This complexity is no doubt related to that seen without any temperature gradient at all²⁴. In that latter case the phase-space distribution is divided into an *infinite* number of coexisting distributions, whose union is Gibbs' canonical distribution ,

$$f_{\text{Gibbs}} = e^{-[q^2 + p^2 + \zeta^2]/2} .$$

The Figures show projections of a strange attractor that forms with $\epsilon = 0.40$. The Lyapunov spectrum in this case is nearly symmetric, so that it is difficult to compute an accurate information dimension of the attractor.

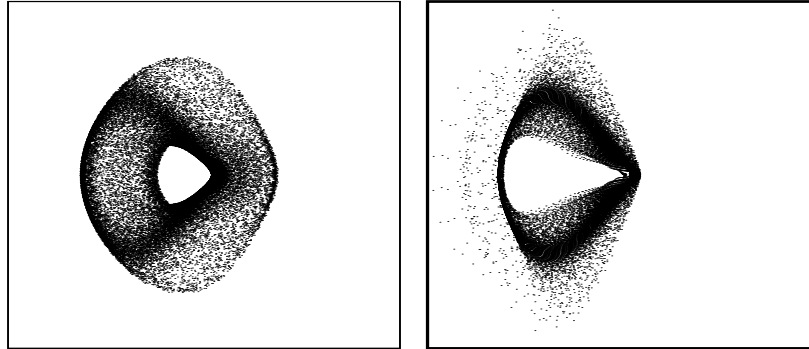
p(left) = 1 ; p(right) = 5



8 x 8 Momentum/Friction Plots

FIG. 4: $\zeta(p)$ for the nonequilibrium Nosé-Hoover oscillator ($\epsilon = 0.4$) is plotted between the limits ± 4 for two different initial conditions. For $p = 5$ the Lyapunov exponents are roughly ± 0.0025 and 0. For $p = 1$ the exponents are much larger in magnitude, ± 0.0085 and 0.

p(left) = 1 ; p(right) = 5



8 x 8 (q,p) Phase-Plane Plots

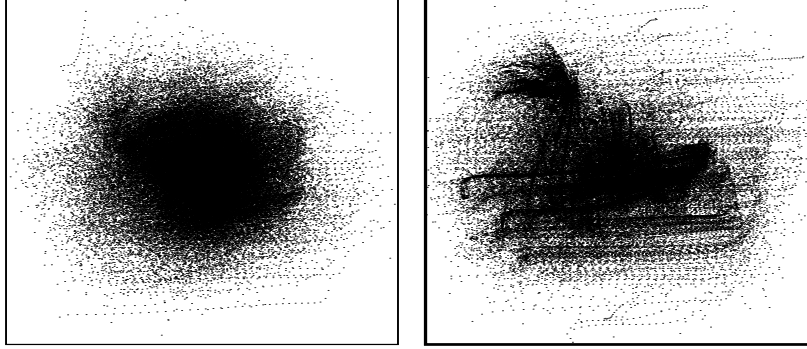
FIG. 5: $p(q)$ is plotted between the limits ± 4 for the two different initial conditions of Figure 4 . Note the preference of the oscillator for the lower-temperature states to the left of the origin.

Fortunately, the complex dynamics of the thermostated oscillator can be greatly simplified by adding another control variable, a friction coefficient controlling the fourth velocity moment²⁶ :

$$\{ \dot{q} = p ; \dot{p} = -q - \zeta p - \xi p^3 ; \dot{\zeta} = p^2 - T(q) ; \dot{\xi} = p^4 - 3p^2 T(q) ; T(q) = 1 + \epsilon \tanh(q) \} .$$

At equilibrium the extra control variable allows the oscillator to sample the complete canonical distribution. This works at nonequilibrium too. Figure 6 compares the distributions of the two friction coefficients (ζ, ξ) for ϵ equal to 0.5 and 1.0 . Even in the latter case the chaos

Temperature Gradients 0.5 and 1.0



10 x 10 x(z) friction coefficients

FIG. 6: Friction coefficient distribution $\xi(\zeta)$ for two values of the maximum temperature gradient, 0.5 and 1.0 . This doubly-thermostated oscillator covers the complete canonical distribution in the equilibrium case. Here there is no dependence of the attractor on the initial value of the momentum. 100,000 points are printed taken from the last half of a 200 million timestep run. The timestep Δt is 0.0002 .

induced by the two coefficients is enough to prevent collapse of the dynamics onto a limit cycle. Although counterintuitive, it appears to be true that a four-dimensional attractor is actually much *simpler* than its three-dimensional counterpart.

A. Larger Systems and Thermodynamics

Larger systems fit the pattern to which the small systems hint. The phase-space distribution shrinks to a strange attractor. In a system with several thermostated degrees of freedom Liouville's Theorem gives the details of the shrinkage^{1,15,26} :

$$(d \ln f / dt) \equiv -(\dot{\otimes} / \otimes) = \sum \zeta \equiv \exp[(\dot{S}/k)] .$$

Here \dot{S} is the external entropy production, the heat extracted from the controlled system by the thermostats, divided by the thermostat temperature. \otimes is a small comoving phase volume. \otimes has three possible evolutions: it can expand; it can shrink; or it can remain the same. The last possibility is the equilibrium one, with no net heat transfer to the outside world. The first possibility (expansion) is ruled out for steady states, as a continually expanding phase volume implies catastrophic instability. Only the possibility of continual shrinkage,

dissipation, is left. The accessible phase-space states for a nonequilibrium steady state continually decrease in number as the volume shrinks (exponentially fast) toward zero. The deterministic time-reversible thermostats make possible a simple geometric interpretation of the Second Law of Thermodynamics. Nonequilibrium steady states necessarily collapse to a zero-volume strange attractor. Thus nonequilibrium states are vanishingly rare. Any attempt to reverse the (time-reversible) dynamics would lead to divergence, with a positive Lyapunov sum, and a violation of the Second Law. What happens in fact is that, when reversed, the dynamics soon breaks its time symmetry and seeks out again the attractor. Time-reversible thermostats have deepened our understanding of the Second Law^{1,27}.

VI. SUMMARY

The paradoxical reversibility properties of Newtonian and Hamiltonian mechanics can be modeled with bit-reversible algorithms. Such algorithms don't exist in cases where the phase volume changes, where the mechanics is thermostated. In the latter case Lyapunov instability seeks out the unstable strange attractor, more stable still than is its repeller twin, leading to a simple geometric understanding of the Second Law of Thermodynamics for open systems.

The symmetry breaking revealed by strong shockwaves suggests that a deepened understanding of isolated systems can come from study of the local Lyapunov spectrum. Both of these problem areas, nonequilibrium conservative systems and nonequilibrium open systems, suggest many interesting research opportunities for the future.

VII. ACKNOWLEDGMENT

This work represents a continuing effort which has been stimulated by many colleagues. Most recently, we thank Francesco Ginelli and Massimo Cencini for inviting our contribution to a special issue of the Journal of Physics A (Mathematical and Theoretical), Lyapunov Analysis from Dynamical Systems Theory to Applications. Anton Krivtsov and Vitaly Kuzkin encouraged our participation in this meeting. We are also specially grateful to Michele Campisi and his colleagues and coworkers for many stimulating emails which helped

us to identify some of the many interesting problem areas presented here.

- ¹ Wm. G. Hoover and C. G. Hoover, *Time Reversibility, Computer Simulation, Algorithms, and Chaos* (World Scientific, Singapore, Second Edition, 2012).
- ² Wm. G. Hoover, *Computational Statistical Mechanics* (Elsevier, Amsterdam, 1991, and available free at <http://www.williamhoover.info>).
- ³ Wm. G. Hoover *Smooth Particle Applied Mechanics: the State of the Art* (World Scientific, Singapore, 2006).
- ⁴ D. Levesque and L. Verlet, “Molecular Dynamics and Time Reversibility”, *Journal of Statistical Physics* **72**, 519-537 (1993).
- ⁵ F. Ginelli, P. Poggi, A. Turchi, H. Chaté, R. Livi, and A. Politi, “Characterizing Dynamics with Covariant Lyapunov Vectors”, *Physical Review Letters* **99**, 130601 (2007).
- ⁶ C. L. Wolfe and R. M. Samelson, “An Efficient Method for Recovering Lyapunov Vectors from Singular Vectors”, *Tellus* **59A**, 355-366 (2007).
- ⁷ M. Romero-Bastida, D. Pázo, J. M. López, and M. A. Rodriguez, “Structure of Characteristic Lyapunov Vectors in Anharmonic Hamiltonian Lattices”, *Physical Review E* **82**, 036205 (2010).
- ⁸ J. D. Farmer, E. Ott, and J. A. Yorke, “The Dimension of Chaotic Attractors”, *Physica* **7D**, 153-180 (1983).
- ⁹ S. D. Stoddard and J. Ford, “Numerical Experiments on the Stochastic Behavior of a Lennard-Jones Gas System”, *Physical Review A* **8**, 1504-1512 (1973).
- ¹⁰ L. B. Lucy, “A Numerical Approach to the Testing of the Fission Hypothesis”, *The Astronomical Journal* **82**, 1013-1024 (1977).
- ¹¹ R. A. Gingold and J. J. Monaghan, “Smoothed Particle Hydrodynamics: Theory and Application to Nonspherical Stars”, *Monthly Notices of the Royal Astronomical Society* **181**, 375-398 (1977).
- ¹² L. D. Landau and E. M. Lifshitz, *Statistical Physics*, equation 33.14 (McGraw-Hill, New Jersey, 1958).
- ¹³ C. Braga and K. P. Travis, “A Configurational Temperature Nosé-Hoover Thermostat”, *Journal of Chemical Physics* **123**, 134101 (2005).
- ¹⁴ L. V. Woodcock, “Isothermal Molecular Dynamics Calculations for Liquid Salts”, *Chemical*

- Physics Letters **10**, 257-261 (1971).
- ¹⁵ B. Moran, Wm. G. Hoover, and S. Bestiale, “Diffusion in a Periodic Lorentz Gas”, Journal of Statistical Physics **48**, 709-726 (1987).
 - ¹⁶ D. J. Evans, W. G. Hoover, B. H. Failor, B. Moran, and A. J. C. Ladd, “Nonequilibrium Molecular Dynamics *via* Gauss’ Principle of Least Constraint”, Physical Review A **28**, 1016-1021 (1983).
 - ¹⁷ S. Nosé, “Constant Temperature Molecular Dynamics Methods”, Progress of Theoretical Physics Supplement **103**, 1-46, (1991).
 - ¹⁸ Wm. G. Hoover, “Mécanique de Nonéquilibre à la Californienne”, Physica A **240**, 1-11 (1997).
 - ¹⁹ C. P. Dettmann and G. P. Morriss, “Hamiltonian Reformulation and Pairing of Lyapunov Exponents for Nosé-Hoover Dynamics”, Physical Review E **55**, 3693-3696 (1997).
 - ²⁰ S. D. Bond, B. J. Leimkuhler, and B. B. Laird, “The Nosé-Poincaré Method for Constant Temperature Molecular Dynamics”, Journal of Computational Physics **151**, 114-134 (1999).
 - ²¹ M. Campisi, F. Zhan, P. Talkner, and P. Hänggi, “Logarithmic Oscillators: Ideal Hamiltonian Thermostats”, arXiv 1203.5968 and 1204.0312 “Reply to W. G. Hoover” (2012) .
 - ²² T. M. Leete, “The Hamiltonian Dynamics of Constrained Lagrangian Systems” [M. S. Thesis, West Virginia University, 1979].
 - ²³ Wm. G. Hoover and C. G. Hoover, “Hamiltonian Dynamics of Thermostated Systems: Two-Temperature Heat-Conducting ϕ^4 Chains”, Journal of Chemical Physics **126**, 164113 (2007).
 - ²⁴ H. A. Posch, Wm. G. Hoover, and F. J. Vesely, “Canonical Dynamics of the Nosé Oscillator: Stability, Order, and Chaos”, Physical Review A **33**, 4253-4265 (1986).
 - ²⁵ Wm. G. Hoover, K. Aoki, C. G. Hoover, and S. V. De Groot, “Time-Reversible Deterministic Thermostats”, Physica D **187**, 253-267 (2004).
 - ²⁶ Wm. G. Hoover, C. G. Hoover, H. A. Posch, and J. A. Codelli, “The Second Law of Thermodynamics and Multifractal Distribution Functions: Bin Counting, Pair Correlations, and the Kaplan-Yorke Conjecture”, Communications in Nonlinear Science and Numerical Simulation **12**, 214-231 (2007).
 - ²⁷ B. L. Holian, Wm. G. Hoover, and H. A. Posch, “Resolution of Loschmidt’s Paradox: the Origin of Irreversible Behavior in Reversible Atomistic Dynamics”, Physical Review Letters **59**, 10-13 (1987).